

Molecular Pathogenesis of Genetic and Inherited Diseases

Defect of Hepatocyte Growth Factor Activator Inhibitor Type 1/Serine Protease Inhibitor, Kunitz Type 1 (Hai-1/Spint1) Leads to Ichthyosis-Like Condition and Abnormal Hair Development in Mice

Koki Nagaike,^{*†} Makiko Kawaguchi,^{*}
Naoki Takeda,[‡] Tsuyoshi Fukushima,^{*}
Akira Sawaguchi,[§] Kazuyo Kohama,^{*}
Mitsuru Setoyama,[¶] and Hiroaki Kataoka^{*}

From the Section of Oncopathology and Regenerative Biology,^{*} Department of Pathology, the Section of Surgical Oncology and Regulation of Organ Function,[‡] Department of Surgery, and the Departments of Anatomy[§] and Dermatology,[¶] Faculty of Medicine, University of Miyazaki, Miyazaki, and the Center for Animal Resources and Development,[‡] Institute of Resources Development and Analysis, Kumamoto University, Kumamoto, Japan

Hepatocyte growth factor activator inhibitor type 1 (HAI-1)/serine protease inhibitor, Kunitz type 1 (SPINT1) is a membrane-bound, serine proteinase inhibitor initially identified as an inhibitor of hepatocyte growth factor activator. It also inhibits matriptase and prostaticin, both of which are membrane-bound serine proteinases that have critical roles in epidermal differentiation and function. In this study, skin and hair phenotypes of mice lacking the *Hai-1/Spint1* gene were characterized. Previously, we reported that the homozygous deletion of *Hai-1/Spint1* in mice resulted in embryonic lethality attributable to impaired placental development. To test the role of Hai-1/Spint1 in mice, the placental function of *Hai-1/Spint1*-mutant mice was rescued. Injection of *Hai-1/Spint1*^{+/+} blastocysts with *Hai-1/Spint1*^{-/-} embryonic stem cells successfully generated high-chimeric *Hai-1/Spint1*^{-/-} embryos (B6*Hai-1*^{-/-High}) with normal placentas. These embryos were delivered without apparent developmental abnormalities, confirming that embryonic lethality of *Hai-1/Spint1*^{-/-} mice was caused by placental dysfunction. However, newborn B6*Hai-1*^{-/-High} mice showed growth retardation and died by 16 days. These mice developed scaly skin because of hyperkeratinization, reminiscent of ichthyosis, and abnormal hair shafts that

showed loss of regular cuticular septation. The inter-follicular epidermis showed acanthosis with enhanced Akt phosphorylation. Immunoblot analysis revealed altered proteolytic processing of profilaggrin in *Hai-1/Spint1*-deleted skin with impaired generation of filaggrin monomers. These findings indicate that Hai-1/Spint1 has critical roles in the regulated keratinization of the epidermis and hair development. (Am J Pathol 2008, 173:1464–1475; DOI: 10.2353/ajpath.2008.071142)

Hepatocyte growth factor activator inhibitor type 1/serine protease inhibitor, Kunitz type 1 (HAI-1/SPINT1) is a serine proteinase inhibitor abundantly expressed in the placenta and epithelial tissues.^{1,2} HAI-1/SPINT1 is synthesized as a type-1 transmembrane protein having two extracellular Kunitz-type serine proteinase inhibitor domains, a transmembrane domain and a short intracytoplasmic domain. A low-density lipoprotein receptor-like domain is present between the two Kunitz domains. The cell surface localization of HAI-1/SPINT1 has been shown immunohistochemically in various epithelial cells, cytotrophoblasts, mesothelial cells, and endothelial cells in human,^{3–6} and HAI-1/SPINT1 regulates proteinase activity on the cell surface.^{7–9} Mouse Hai-1/Spint1 also shows similar expression patterns to that of human.¹⁰ In addition, ectodomain shedding of HAI-1/SPINT1 was also observed to possibly regulate proteinase activities in pericellular spaces.^{7,11}

Supported by the Ministry of Education, Science, Sports, and Culture of Japan [grants-in-aid for scientific research (B) no. 14370079 and no. 20390114].

K.N., M.K., and N.T. contributed equally to this study.

Accepted for publication July 29, 2008.

Address reprint requests to Hiroaki Kataoka, M.D., Ph.D., Section of Oncopathology and Regenerative Biology, Department of Pathology, Faculty of Medicine, University of Miyazaki, 5200 Kihara, Kiyotake, Miyazaki 889-1692, Japan. E-mail: mejina@med.miyazaki-u.ac.jp.

To date, several serine proteinases have been proposed as target enzymes of HAI-1/SPINT1. These include hepatocyte growth factor activator (HGFA), matriptase (also known as membrane-type serine proteinase 1), prostaticin, and hepsin.^{1,2,12-14} HGFA is a serum proteinase known to activate hepatocyte growth factor/scatter factor (HGF).^{2,15} On the other hand, matriptase, prostaticin, and hepsin are membrane-associated serine proteinases that act on the cellular surface.¹⁶ Recent studies have revealed that interaction between matriptase and prostaticin appears to have an important proteolytic cascade regulating terminal epidermal and hair follicle differentiation,¹⁷ and knocking out of either *matriptase* (*St14*) or *prostaticin* (*Prss8*) results in severe skin phenotypes showing impaired epidermal barrier function, abnormal processing of profilaggrin, and immature hair follicles in mice.^{18,19} Therefore, Hai-1/Spint1 might have a central role in differentiation of the epidermis and hair follicle by interacting with matriptase and prostaticin. In addition to the roles in normal skin development and homeostasis, a recent study has suggested that matriptase has a critical role in skin carcinogenesis, and consequently, Hai-1/Spint1 may serve as a suppressor of matriptase-induced skin cancer.²⁰ Moreover, significant roles of matriptase and hepsin in progression of cancers in other organs are also reported.²¹⁻²³

Previously we reported that the targeted disruption of *Hai-1/Spint1* in mice resulted in embryonic lethality and impaired placental development with a defect of the labyrinthin layer.¹⁰ The placental defect in *Hai-1/Spint1*^{-/-} mice was also confirmed by other studies, and this phenotype was likely to be caused by deregulated pericellular proteolysis attributable to disturbance of the balance between Hai-1/Spint1 and its target proteinase, particularly matriptase.^{24,25} These observations suggest that pericellular interactions of proteinases and proteinase inhibitors have critical roles in tissue morphogenesis and development. However, intrauterine lethality of *Hai-1/Spint1*^{-/-} embryos seriously impaired the exploration of physiological and pathological functions of Hai-1/Spint1 *in vivo*. In this study, to overcome this restriction and to study the role of Hai-1/Spint1 in embryos, we attempted to avoid placental dysfunction of *Hai-1/Spint1*^{-/-} mice. To this end, we established homozygous *Hai-1/Spint1*^{-/-} murine embryonic stem (ES) cell lines of C57BL/6 background and microinjected them into *Hai-1/Spint1*^{+/+} blastocysts to obtain high-chimerism embryos almost lacking Hai-1 expression (*B6Hai-1*^{-/-High}) with wild-type (*Hai-1/Spint1*^{+/+}) placentas. As expected, the normal placental function rescued Hai-1/Spint1-deficient embryos from intrauterine death. However, *B6Hai-1*^{-/-High} pups showed significant skin abnormalities.

Materials and Methods

Generation of Homozygous *Hai-1/Spint1*-Deleted ES Cells and Genotyping

Generation of *Hai-1/Spint1*-disrupted mice was described previously.¹⁰ Homozygous *Hai-1/Spint1*-deleted

ES cells (*B6Hai-1*^{-/-} ES) from 3.5 days postcoitum (dpc) were generated from pregnant *Hai-1/Spint1* heterozygous females mated to *Hai-1/Spint1* heterozygous males, both of which had been backcrossed to C57BL/6. These cell lines were genotyped by polymerase chain reaction (PCR) and Southern blot analysis. Genomic DNA was obtained from ES cells by proteinase K digestion followed by phenol-chloroform-isoamylalcohol extraction and ethanol precipitation. The isolated DNA was subjected to PCR for 45 cycles using primers for the wild-type allele (forward, 5'-GAGGTTGCCTGGGCAACAAGAACA-3' and reverse, 5'-GAAGCCATCGATACAGCAGCATTG-3'), and for the mutant allele (forward, 5'-AGAAAACGTCCGGAAGAAGTGGAGC-3', and reverse, 5'-ATTAAGGGTTCGGATCCTCTAGAGTCGAG-3') to detect a 588-bp product for the wild-type allele and a 280-bp product for the mutant allele. Southern blotting was performed following the protocol provided in the AlkPhos direct labeling and detection system (GE Health Care, Buckinghamshire, UK). In brief, 10 μ g of genomic DNA was digested with *Hind*III (New England Biolabs, Ipswich, MA), separated by electrophoresis on a 0.8% agarose gel, and transferred to Hybond N⁺ nylon membranes (GE Health Care), followed by overnight hybridization at 55°C to the probe (800 bp), which was prepared by PCR using mouse genomic DNA as a template. Primer sequences for the probe were forward (5'-GTGTTTCCTGGGCATCAAGCTCAG-3') and reverse (5'-GGGATGTAACAGGAGAGGTCTGAG-3'). After stringent washing according to the manufacturer's instructions, signal was detected by exposing the Hyperfilm ECL reagent (GE Health Care) to the membrane for 3 hours in a dark room.

Production of *B6Hai-1*^{-/-} ES Cell and ICR or Ayu8104 Embryo Chimeras

Ayu8104/LacZ mice (B6; CB-Cdk6^{GtAyu8104Imeg}) were provided by the Center for Animal Resources and Development (Kumamoto, Japan). This mouse was backcrossed with CBA twice (Ayu8104/CBA/LacZ), and then intercrossed with ICR (Ayu8104/ICR/LacZ). Both Ayu8104/CBA/LacZ (agouti color) and Ayu8104/ICR/LacZ (white color) were used for chimera generation. Chimeras were generated by injection of *B6Hai-1*^{-/-} ES cells into blastocysts isolated from *Hai-1/Spint1*^{+/+} ICR, *Hai-1/Spint1*^{+/+} Ayu8104/CBA/LacZ, or *Hai-1/Spint1*^{+/+} Ayu8104/ICR/LacZ, and transferred to pseudo-pregnant ICR females (2.5 dpc). Wild-type C57BL/6 *Hai-1/Spint1*^{+/+} mice and C57BL/6 *Hai-1/Spint1*^{+/-} heterozygous mice were used as controls. In addition, heterozygous ES cells (*B6Hai-1*^{+/-}) were also used to generate chimeras and the resultant high-chimerism heterozygous mice (*B6Hai-1*^{+/-High}) were also used as controls. The extent of chimerism was judged by genotyping by PCR, neonate hair color, LacZ staining, and also by immunohistochemical analysis of Hai-1/Spint1 protein. In an indicated experiment, recipients were sacrificed at term to recover the embryos. The embryos were then genotyped and submitted for histological analysis. For PCR, genomic DNA was obtained from the embryo or tail using

the Wizard DNA purification kit (Promega Inc., Madison, WI) according to the manufacturer's instructions and subjected to PCR as described above. All experiments were approved by the Animal Care and Use Committee of the University of Miyazaki.

LacZ Staining

Embryos and placentas from B6*Hai-1*^{-/-} ES cells and Ayu8104 blastocyst chimeric mice were fixed in 1% formaldehyde, 0.2% glutaraldehyde, and 0.02% Nonidet P-40 in phosphate-buffered saline (PBS). LacZ activity was detected for 16 hours in developing solution (1 mg/ml X-gal, 5 mmol/L K₃Fe(CN)₆, 5 mmol/L K₄Fe(CN)₆, and 2 mmol/L MgCl₂ in PBS) after preincubation in PBS for 1 hour at 50.5°C. LacZ-stained embryos and placentas from fresh-frozen sections were incubated in developing solution, and alternate sections were stained with hematoxylin and eosin (H&E). Embryos were genotyped by PCR using yolk sac DNA as described above.

Reverse Transcriptase-Polymerase Chain Reaction (RT-PCR)

Total RNA was prepared with TRIzol (Invitrogen Japan, Tokyo, Japan) followed by DNase I (Takara Bio, Otsu, Japan) treatment. For RT-PCR, 3 µg of total RNA was reverse-transcribed with a mixture of oligo (dT)₁₂₋₁₈ (Invitrogen Japan) and random primers (6 mer) (Takara Bio) using 200 U of ReverTraAce (Toyobo, Osaka, Japan), and 1/30 of the resultant cDNA was processed for each PCR reaction with 0.1 µmol/L of both forward and reverse primers and 2.5 U of HotStar TaqDNA polymerase (Qiagen, Tokyo, Japan). The following primers were used: *Hai-1/Spint1*, forward (5'-GCTGTGCCCGATTACCTATG-3') and reverse (5'-GACCACTATGATGCAGATGACCAGA-3'); *matriptase* (St14, GenBank accession no. NM011176), forward (5'-CACGAATGATGTGTGTGGGTTTC-3') and reverse, (5'-CCTGGAACATTCGCCCATCT-3'); *β-actin*, forward (5'-TGACAGGATGCAGAAGGAGA-3') and reverse (5'-GCTGGAAGGTGGACAGTGAG-3').

Histology, Immunohistochemistry, and Electron Microscopy

Embryo and placenta tissue were fixed in 4% paraformaldehyde-PBS overnight and then dehydrated and embedded in paraffin. Four-µm-thick sections were prepared and stained with H&E. For immunohistochemistry, the sections were processed for antigen retrieval (autoclaved in 10 mmol/L citrate buffer, pH 6.0 for 5 minutes), followed by treatment with 3% H₂O₂ in PBS for 10 minutes, and washed in PBS twice. After blocking in 3% bovine serum albumin and 10% normal goat serum in PBS for 1 hour at room temperature, the sections were incubated with primary antibodies for 16 hours at 4°C. The preparation of anti-mouse *Hai-1/Spint1* rabbit polyclonal antibody was described previously.²⁶ Anti-phosphorylated Akt rabbit monoclonal antibody (Cell Signaling Technology, Dan-

vers, MA), anti-Ki-67 rat monoclonal anti-mouse antibody (clone TEC-3; DAKO, Glostrup, Denmark), and anti-cleaved caspase-3 rabbit polyclonal antibody (Cell Signaling Technology) were also used. Negative controls consisted of omission of the primary antibody. The sections were then washed in PBS and incubated with Envision-labeled polymer reagent (DAKO) or with Histofine Simple Stain Mouse MAX-PO reagent (Nichirei, Tokyo, Japan) for 45 minutes at 37°C. The reaction was revealed with nickel, cobalt-3,3'-diaminobenzidine (Immunopure metal enhanced DAB substrate kit; Pierce, Rockford, IL) and the sections were counterstained with hematoxylin.

For electron microscopy, specimens were fixed with a mixture of 2% paraformaldehyde and 2.5% glutaraldehyde in 0.1 mol/L phosphate buffer, pH 7.4. After rinsing with the buffer, the specimens were postfixed with 1% osmium tetroxide in 0.1 mol/L phosphate buffer for 2 hours at 4°C. For scanning electron microscopy, after washing with distilled water, they were dehydrated in a graded ethanol series, and then freeze-dried in a t-butanol freeze-drying apparatus (ID-2; Eiko, Tokyo, Japan). Dried specimens were coated with platinum in a sputter-coating machine (E-102; Hitachi, Tokyo, Japan) and observed in a Hitachi S-4800 scanning electron microscope. For transmission electron microscopy, postfixed specimens were washed with distilled water, and then dehydrated through a graded ethanol series, substituted with propylene oxide, and embedded in epoxy resin. Ultrathin (80 nm thickness) sections were cut and stained with 2% uranyl acetate in 70% methanol for 4 minutes followed by Reynolds' lead citrate for 3 minutes, and observed in a JEOL 1200EX (JEOL, Tokyo, Japan) transmission electron microscope.

Analysis of Epidermal Barrier Function

To check the loss of water across the skin, dehydration assay was performed according to the method described previously.¹⁸ Newborn mice were obtained by caesarian section at embryonic day 18.5 (E18.5), resuscitated, separated from their mother to prevent fluid intake, and placed in a 37°C incubator. The rate of epidermal fluid loss was calculated by measuring the reduction of body weight throughout a period of 6 hours.

Culture of Primary Murine Keratinocytes

Primary murine keratinocytes were prepared and propagated as described²⁷ with minor modifications. Briefly, the epidermis of sacrificed newborn wild-type and chimera mice (1 to 3 days old) were separated from the dermis after collagenase digestion overnight. Keratinocytes separated by collagenase digestion were seeded in keratinocyte growth medium (Cell Applications, San Diego, CA). Experiments were performed after 5 to 6 days of cell culture with media changes every second day. Keratinocyte basal medium (Cell Applications) was used as starvation medium.

Immunoblot Analysis

To detect phospho-Akt and Akt, keratinocyte cellular proteins were extracted on ice in cell lysis buffer (CellLytic-M; Sigma, St. Louis, MO) supplemented with protease inhibitor cocktail (Sigma), 100 mmol/L NaF, and 1 mmol/L Na₃VO₄. After centrifugation at 16,000 × *g* for 15 minutes at 4°C, equal amounts of total proteins were separated by sodium dodecyl sulfate (SDS)-polyacrylamide gel electrophoresis (PAGE) under reducing conditions using 4 to 12% gradient gels and transferred onto Immobilon membrane (Millipore, Bedford, MA). After blocking with 1% phosphatase-free bovine serum albumin in Tris-buffered saline with 0.05% Tween 20 (TBS-T), the membranes were incubated with primary antibody at 4°C overnight, followed by washing in TBS-T and incubation with horseradish peroxidase-conjugated swine anti-rabbit IgG (DAKO) diluted in TBS-T with 1% bovine serum albumin for 1 hour at room temperature. The labeled proteins were visualized with a chemiluminescence reagent (PerkinElmer Life Science, Boston, MA). The keratinocyte culture-conditioned media and extracts, and tissue extracts of mouse skin were also used for detection of profilaggrin processing, matriptase, and prostaticin. To detect profilaggrin processing and prostaticin in the skin, mouse tissues were homogenized on ice in lysis buffer containing 50 mmol/L Tris-HCl (pH 8.0), 150 mmol/L NaCl, 0.2% Nonidet P-40, 0.5% sodium deoxycholate, 0.1% SDS, and protease inhibitor cocktail (Sigma). The extracts were centrifuged at 25,000 × *g* for 20 minutes at 4°C, and the resulting supernatants were used for experiments. To detect HGF processing in the skin, mouse tissue was homogenized in 4 vol of ice-cold extraction buffer containing 50 mmol/L Tris-HCl, pH 7.5, 0.15 mol/L NaCl, proteinase inhibitor cocktail (Sigma), and 0.01% 3-[(3-cholamidopropyl)dimethylammonio]propane-1-sulfonic acid, followed by centrifugation (25,000 × *g* for 15 minutes). The resultant supernatants were mixed with heparin-Sepharose beads (Pharmacia, Uppsala, Sweden) in the presence of 100 μmol/L nafamostat mesilate (Torii Pharmaceutical Co., Tokyo, Japan). After the Sepharose beads had been washed three times with PBS, bound HGF was eluted with SDS-PAGE sample buffer and boiled for 3 minutes. Primary antibodies were as follows: anti-phospho-Akt mouse monoclonal antibody (Ser473) at 1:1000 dilution, anti-Akt rabbit monoclonal antibody (Cell Signaling Technology) at 1:1000 dilution, anti-filaggrin rabbit polyclonal antibody (Covance, Richmond, CA) at 1:10000 dilution, anti-prostaticin mouse monoclonal antibody (BD Bioscience PharmMingen, San Diego, CA) at 1:250 dilution, anti-mouse HGF rabbit polyclonal antibody (R&D Systems, Minneapolis, MN) at 1:2000 dilution. For detection of prostaticin, mouse True Blot Western blot kit (Bay Bioscience, Kobe, Japan) was used according to the manufacturer's instructions.

Casein Gel Zymography

Casein zymography was performed using serum-free conditioned media of cultured mouse keratinocytes. The

cells were cultured in serum-free keratinocyte growth medium (Cell Applications) for 2 days and the conditioned media were collected, centrifuged to remove cell debris, dialyzed overnight at 4°C, and lyophilized. The dried protein powder was dissolved in a 1/20 vol of the initial conditioned media in 20 mmol/L Tris-HCl (pH 7.5). The concentrated media were electrophoresed in 10% SDS-polyacrylamide gels impregnated with 1 mg/ml of casein. Samples were mixed with SDS-PAGE sample buffer without boiling and electrophoresed under nonreducing conditions. After electrophoresis, gels were washed in 50 mmol/L Tris-HCl (pH 7.5) containing 0.1 mol/L NaCl, 2.5% Triton X-100 for 1.5 hours to remove SDS, followed by incubation in 50 mmol/L Tris-HCl at pH 7.5, 0.5 mmol/L ethylenediaminetetraacetic acid) containing 10 μmol/L broad-spectrum metalloprotease inhibitor GM6001 (Millipore) for 30 minutes to eliminate matrix metalloproteinase activities. The gels were incubated at 37°C for 72 hours in 50 mmol/L Tris-HCl (pH 7.5), and stained with Coomassie Brilliant Blue.

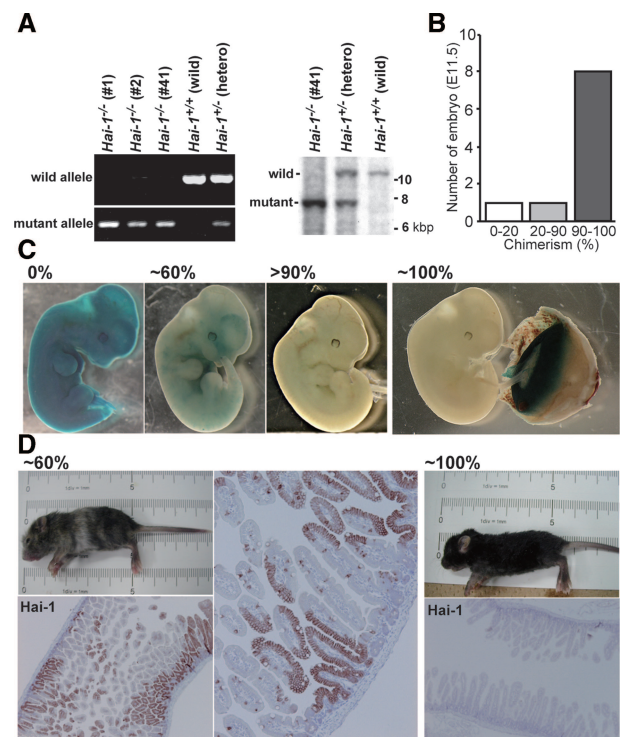


Figure 1. Establishment of B6*Hai-1*^{-/-} ES cells and generation of embryo chimeras. **A:** Genotyping of ES cells in C57BL/6 background. Representative results of PCR and Southern blot analysis are shown. In the PCR study, 588-bp and 280-bp products for wild-type allele and mutant allele, respectively, were detected. In Southern blot analysis, 10.3-kbp product and 7.7-kbp fragments for wild-type allele and mutant allele, respectively, were detected. **B:** Efficiency of chimera production. Chimeras were generated by injection of B6*Hai-1*^{-/-} ES 1 cells into blastocysts isolated from Ayu8104/ICR/LacZ mouse. The extent of chimerism of each embryo (E11.5) was judged by LacZ staining. **C:** Representative results of LacZ staining of embryo (E11.5) of B6*Hai-1*^{-/-} ES 1-Ayu8104/ICR/LacZ blastocyst chimera. The placenta tissue of ~100% B6*Hai-1*^{-/-} ES 1 chimera embryo showed strong LacZ staining, confirming that the placenta tissue was in fact derived from *Hai-1*/*Spint1*^{+/+} Ayu8104/ICR/LacZ. **D:** Evaluation of the extent of chimerism by hair color and Hai-1/Spint1 immunostain. The intestinal tissue was immunostained with anti-Hai-1/Spint1 antibody. The extent of chimerism in the intestinal tissue was proportional to the chimerism judged by the coat color.

Statistical Analysis

Data are presented as mean ± SD. Comparison between two unpaired groups was done with repeated measure analysis of variance or Mann-Whitney *U*-tests. Significance was set at *P* < 0.05. All statistical analysis was performed using Statview 5.0 program (Brainpower Inc., Calabasas, CA).

Results

Establishment of *B6Hai-1^{-/-}* ES Cells and Generation of Embryo Chimeras

We established five ES cell lines of C57BL/6 background with homozygous deletion of *Hai-1/Spint1* from pregnant *Hai-1/Spint1* heterozygous females mated to *Hai-1/Spint1* heterozygous males. Among them, three ES lines, namely *B6Hai-1^{-/-}* ES 1, 2, and 41 (Figure 1A), were able to generate embryo chimeras. By injection of *B6Hai-1^{-/-}* ES cells in blastocysts derived from Ayu8104/CBA/LacZ, Ayu8104/ICR/LacZ, or ICR mice, we successfully generated embryos of very high chimerism, in which the expression of *Hai-1/Spint11* was mostly deleted (*B6Hai-1^{-/-High}*)

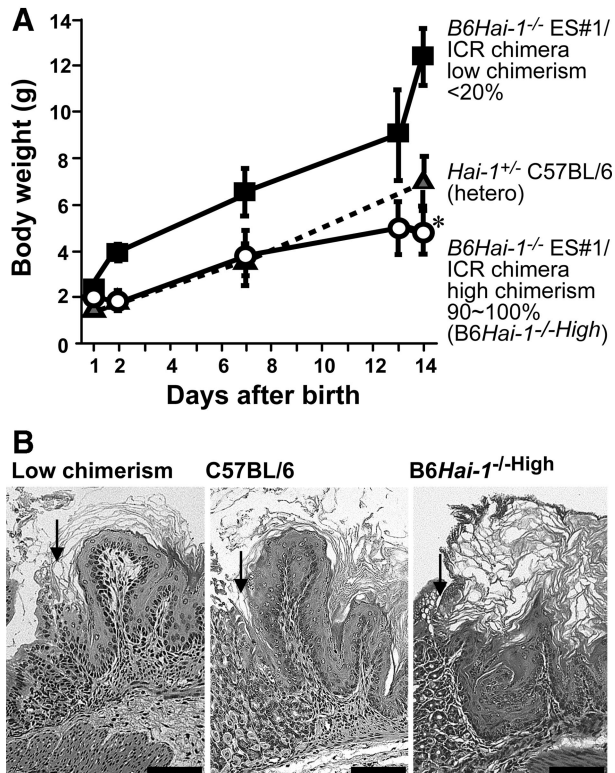


Figure 2. Growth of the neonatal chimera mice and histology of the forestomach. **A:** Body weight gain of *B6Hai-1^{-/-High}* pups. For controls, *Hai-1/Spint1^{+/-}* heterozygous mice in C57BL/6 background and low-chimerism mice were also analyzed (*n* = 5, for each group). Each value represents mean ± SD. **P* < 0.05 and *P* < 0.001 compared with hetero mice and low-chimerism mice, respectively. **B:** Histology of the forestomach (H&E stain). The forestomach of *B6Hai-1^{-/-High}* shows extensive keratinization. Arrows indicate the junction between forestomach and glandular stomach. Scale bar = 100 μm.

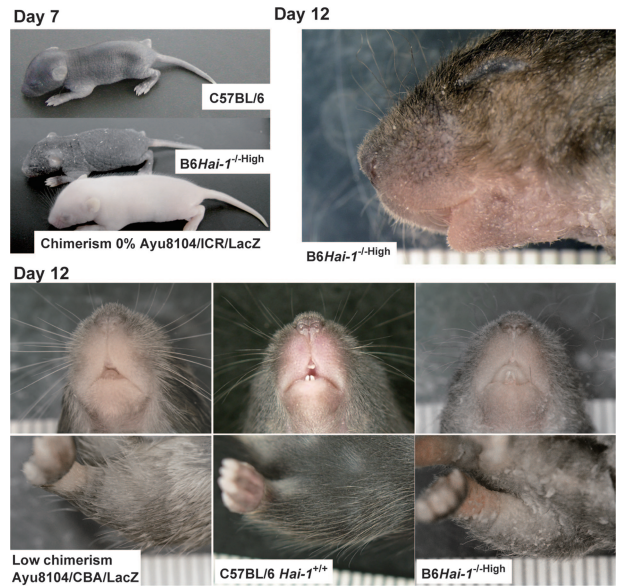


Figure 3. External appearance of newborn mice. Scaly skin became apparent at day 7 in *B6Hai-1^{-/-High}*, compared with wild-type mice. At day 12, scaly skin is evident with abnormally curved hair and whiskers.

and *Hai-1/Spint1^{+/-}* placentas developed normally. In case of the Ayu8104/LacZ-derived blastocysts, the chimerism of the embryo was confirmed by LacZ staining. Eight of ten embryos showed 90 ~ 100% chimerism (Figure 1B). Representative results of LacZ staining are shown in Figure 1C. As expected, normal placental function rescued *Hai-1/Spint1^{-/-}* embryos from embryonic lethality, confirming the hypothesis that embryonic lethality of *Hai-1/Spint1^{-/-}* is primarily caused by impaired placental development. The delivery of *B6Hai-1^{-/-High}* pups was also observed by injection of *B6Hai-1^{-/-}* ES cells into ICR blastocysts. In this case, the chimerism and extent of *Hai-1/Spint1* deletion were confirmed by mouse coat color and *Hai-1/Spint1* protein immunostain of the intestinal mucosa that normally expresses considerable levels of *Hai-1/Spint1* (Figure 1D).

The delivered *B6Hai-1^{-/-High}* pups were viable and did not show any visible anomalies at birth. However, several days after birth, growth retardation became apparent, and the mice died within 16 days after birth (Figure 2A). Autopsy did not reveal apparent anomalies in visceral organs, except for enhanced keratinization of the forestomach epithelium (Figure 2B) and increased extramedullary hematopoiesis in the liver, compared with wild-type mice. In contrast to the forestomach, the esophageal stratified squamous epithelium did not show hyperkeratinization (data not shown). On the other hand, significant differences were observed in the skin of *B6Hai-1^{-/-High}* mice.

Skin Abnormalities in *Hai-1/Spint1*-Deleted Mice

As shown in Figure 3, *B6Hai-1^{-/-High}* mice became scaly, with considerable amounts of hyperkeratotic scales on the skin surface, reminiscent of ichthyosis.

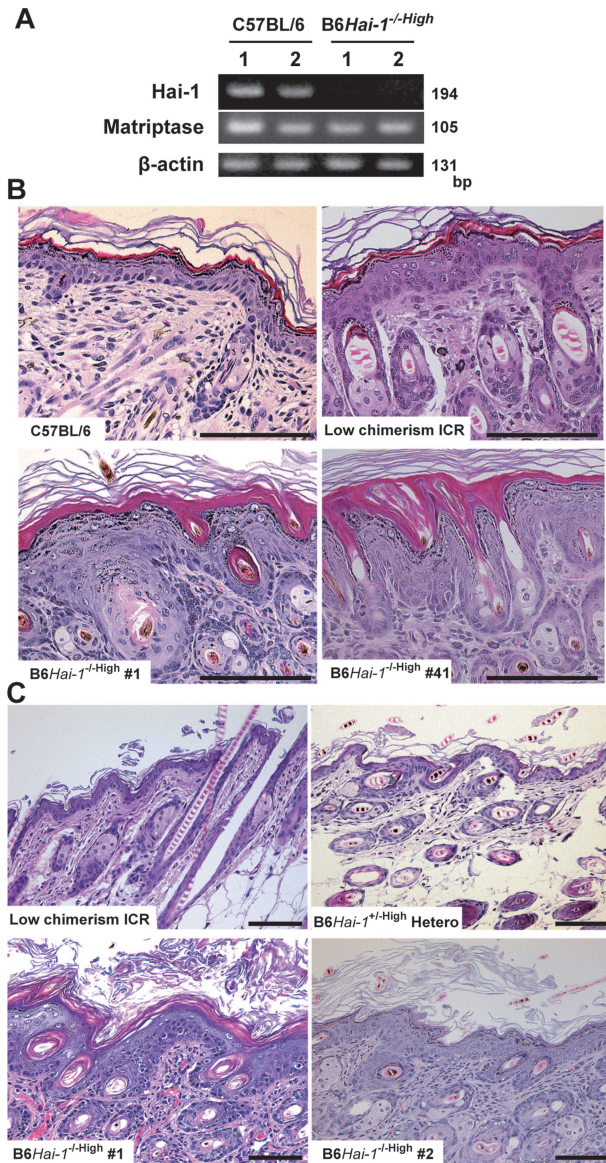


Figure 4. Histology of skin abnormalities in *Hai-1/Spint1*-deleted mice at 7th day after birth. **A:** Expression of Hai-1/Spint1 and matriptase in the skin. Hai-1/Spint1 mRNA was undetectable in *B6Hai-1^{-/-High}* skin derived from chimera generated by injection of *B6Hai-1^{-/-}* ES 41 cells into *Hai-1/Spint1^{+/+}* ICR blastocysts even with sensitive RT-PCR study (35 cycles of amplification). In contrast, wild-type skin tissue shows Hai-1/Spint1 expression. Matriptase expression was equally observed in both groups. Results from two mice were shown in each group. **B:** Histology of the dorsal skin (H&E stain). *B6Hai-1^{-/-High}* epidermis shows hypergranulosis with thick stratum corneum. Note that *B6Hai-1^{-/-}* ES 1 and *B6Hai-1^{-/-}* ES 41 resulted in the same epidermal abnormalities in high-chimerism mice. **C:** Histology of skin abnormalities at 14th day after birth. In *B6Hai-1^{-/-High}* mouse, the external surface of the dorsal skin was covered by a thick desquamating keratin layer, and the epidermis showed acanthosis with mildly enlarged keratinocyte nuclei compared with that of low-chimerism mice or high-chimerism mice generated by *B6Hai-1^{+/+}* (hetero) ES cells and ICR blastocysts (*B6Hai-1^{+/+High}* Hetero). H&E stain. Scale bars = 100 μ m.

Their hair and whiskers were thin and sparse. These external abnormalities were equally observed in chimeras generated by using blastocysts isolated from *Hai-1/Spint1^{+/+}* ICR, *Hai-1/Spint1^{+/+}* Ayu8104/CBA/LacZ, and *Hai-1/Spint1^{+/+}* Ayu8104/ICR/LacZ (Figure 3). RT-PCR confirmed that Hai-1/Spint1 mRNA was undetectable in *B6Hai-1^{-/-High}* skin (Figure 4A). The level of matriptase

Table 1. Thickness of Keratinized Layer

Mice	Thickness
Chimerism 90 ~ 100% (<i>B6HAI-1^{-/-High}</i>) (<i>n</i> = 15)	247 \pm 101 μ m*
Chimerism 40 to 60% (C57BL/6-ICR) (<i>N</i> = 3)	70 \pm 49 μ m
Chimerism <20% (ICR background) (<i>n</i> = 6)	23 \pm 9 μ m
Heterozygous mice (<i>B6HAI-1^{+/-High}</i>) (<i>n</i> = 4)	45 \pm 53 μ m

Thickness of keratin layer was measured at 10 randomly selected portions of dorsal skin in each mouse. Values are mean \pm SD.
 **P* < 0.005 compared with other groups.

mRNA, a possible cognate enzyme of Hai-1/Spint1 in the skin, was not apparently altered in the Hai-1/Spint1-deficient skin (Figure 4A). Histologically, at 1 week after birth, the epidermal stratum corneum was abnormally packed and thick in *B6Hai-1^{-/-High}* mice compared with control C57BL/6 and low-chimerism mice (Figure 4B). Within 10 days of birth, acanthosis of the epidermis became apparent, and at 2 weeks after birth, the epidermis of *B6Hai-1^{-/-High}* was covered by a thick layer of desquamating keratin and was apparently thicker than that of control mice (Figure 4C). The granular layer was preserved well in the mutant epidermis. Neutrophilic infiltration was occasionally observed in the dermis of *B6Hai-1^{-/-High}* mice and the mice showed significant growth retardation. The mean thickness of the keratinized layer of *B6Hai-1^{-/-High}* skin was approximately five times thicker than that of control mice (Table 1). It should be emphasized that all three *B6Hai-1^{-/-}* ES clones (no. 1, 2, and 41) resulted in the same skin phenotype whenever high chimerism was achieved.

The skin phenotype observed in *B6Hai-1^{-/-High}* mice suggested a possibility of abnormal barrier function of the skin. To test the barrier function of Hai-1/Spint1-deficient epidermis, the rate of fluid loss through transepidermal evaporation was determined in *B6Hai-1^{-/-High}* mice and control C57BL/6 newborn mice obtained by caesarian section at E18.5. The newborn litters were separated from their mothers and the loss of fluids at 37°C was recorded for each individual pup throughout a 6-hour period by monitoring the body weight. As shown in Figure 5, the inward-out barrier function of *B6Hai-1^{-/-High}* epidermis was compromised compared to that of C57BL/6 pups. The rate of fluid loss of *B6Hai-1^{-/-High}* mice was 1.5- to 2-fold higher than control mice and the difference was statistically significant (*P* < 0.005, repeated measure analysis of variance).

Localization of Hai-1/Spint1 in Mouse Skin

Because skin phenotypes were evident in *B6Hai-1^{-/-High}* mice, we tested the expression of Hai-1/Spint1 protein in normal mice skin (C57BL/6 and ICR). Consistent with the above findings, Hai-1/Spint1 protein was strongly expressed in hair cortex and cuticle cells of anagen hair

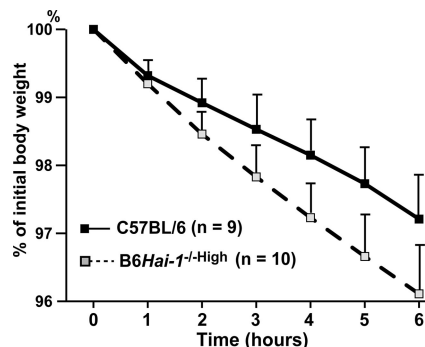


Figure 5. Reduced barrier function of Hai-1/Spint1-deficient epidermis. Newborn mice were obtained by caesarian section at E18.5, resuscitated, separated from their mother to prevent fluid intake, and placed in a 37°C incubator. The rate of epidermal fluid loss was calculated by measuring the reduction of body weight. The values are means \pm SD. The time course difference between two groups was statistically significant ($P < 0.005$, repeated measure analysis of variance).

follicles and to a lesser degree in the primary hair germ (Figure 6, A–C). This strong expression pattern of Hai-1/Spint1 in hair cortex cells resembled that of matriptase,²⁸ a cognate proteinase of Hai-1/Spint1.¹² The Hai-1/Spint1 immunoreactivity was also noted in the epidermis, and transitional cells between granular and corny layers showed strong expression pattern (Figure 6, A and B), which was similar to matriptase and prostaticin.^{28,29} The Hai-1/Spint1 immunoreactivity in epidermal keratinocytes was weak at 1 or 2 weeks after birth, occasionally showing cytoplasmic reactivity (Figure 6C). Because the antibody recognized intracytoplasmic domain of Hai-1/Spint1, this cytoplasmic reactivity may represent internalized Hai-1/Spint1 fragment after ectodomain shedding as described previously.²⁶ As expected, no Hai-1/Spint1 immunoreactivity was observed in the skin of B6Hai-1^{-/-}High mice. The hair bulbs of dorsal skin may be modestly enlarged in Hai-1/Spint1-deficient skin compared with control C57BL/6 skin (Figure 6D).

Impaired Formation of Regular Cuticle Layer in Hai-1/Spint1-Deficient Hair and Whisker

Scanning electron microscopy of the hair and whiskers revealed undulating shape with fragile appearance in B6Hai-1^{-/-}High mice (Figure 6, E and F). Notably, the Hai-1/Spint1-deficient whisker had an indistinct or poor quality cuticle. A well-defined and regular cuticular septation observed in normal whisker surface was absent in the mutant whiskers (Figure 6G). The ichthyosis-like change showing thick layers of hyperkeratotic scale covering on the skin surface was also confirmed with scanning electron microscopy (Figure 6H). The impaired formation of regular layered structure of cuticle was clearly indicated by transmission electron microscopy (Figure 7). The cuticle structure consisted of a series of lamination in normal whisker. However, in Hai-1/Spint1-deficient whisker, malformation of the cuticle layer is evident, showing irregular exocuticle/endocuticle boundary with complete

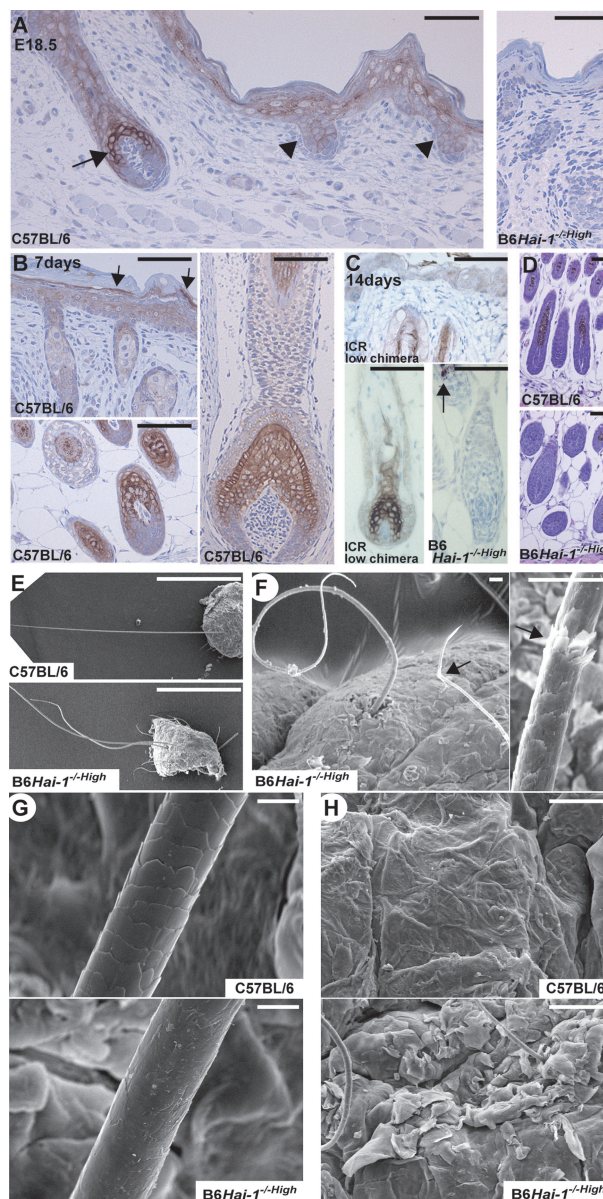


Figure 6. Abnormalities of hair and whiskers in Hai-1/Spint1-deleted mice. **A:** Expression and localization of Hai-1/Spint1 protein in wild-type skin (C57BL/6) at E18.5. Hai-1/Spint1 is strongly expressed by hair cortex cells of early anagen hair follicle (arrow). It is also expressed in epidermal keratinocytes, especially in the granular layer, and to a lesser degree by primary hair germ (arrowheads). The skin of Hai-1/Spint1-deleted mouse (B6Hai-1^{-/-}High, E18.5) was simultaneously immunostained as a control (right). **B:** Expression of Hai-1/Spint1 in wild-type skin at day 7. Hai-1/Spint1 is strongly expressed by hair cortex and cuticle cells and weakly by inner root sheath of follicles (bottom left, dorsal skin pelage hair follicles; right, whisker follicle). In the epidermis, immunoreactivity for Hai-1/Spint1 is also observed and the expression appears to be most evident in transitional cells between granular and corny layers (arrows). **C:** Expression of Hai-1/Spint1 in wild-type skin (ICR, chimerism 0%) at day 14. Hai-1/Spint1 is strongly expressed by hair cortex cells of anagen hair follicle. No immunoreactivity was detectable in B6Hai-1^{-/-}High hair follicles. Arrow indicated melanin pigments of black hair. **D:** Histology (H&E) of anagen hair follicles of dorsal skin pelage hair at 1 week after birth. **E–H:** Scanning electron microscopy images of whiskers and hair (E–G) and skin surface (H) of wild-type (C57BL/6) and B6Hai-1^{-/-}High mice. Fragile appearance (F, arrows) and poorly formed cuticle layer (G) are observed in B6Hai-1^{-/-}High mouse. Scale bars: 1 mm (E); 20 μ m (F); 10 μ m (G); 50 μ m (A–D, H).

defect of normal laminated structure. This cuticular defect may account for the fragile appearance of mutant hair and whiskers.

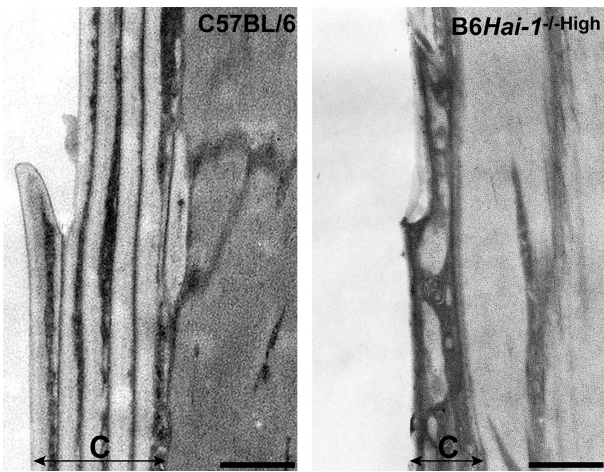


Figure 7. Transmission electron microscopy of cuticle layer of whisker surface (7th day). Regular layered structure of cuticle (C) is severely impaired in *Hai-1/Spint1*-deleted whisker. Scale bar = 0.5 μm .

Altered Filaggrin Processing in Keratinocytes of *B6Hai-1^{-/-High}* Mice

To test whether matriptase activity was in fact altered in the skin of *B6Hai-1^{-/-High}* mice because of deficient Hai-1/Spint1 activity, profilaggrin processing was examined.³⁰ Detergent extracts of skin from *B6Hai-1^{-/-High}*, low-chimerism mice (<20%), and control *C57BL/6Hai-1^{+/+}* mice were subjected to immunoblot analysis for filaggrin. The results revealed altered processing of profilaggrin, showing increased filaggrin dimer and trimer in *B6Hai-1^{-/-High}*. However, the generation of filaggrin monomer was markedly decreased in the *Hai-1/Spint1*-deleted skin compared with control *C57BL/6Hai-1^{+/+}* mice and low-chimerism mice (Figure 8A). Moreover, an abnormally processed filaggrin band that was ~6 kDa smaller than the filaggrin dimer was abundantly observed in *Hai-1/Spint1*-deleted skin (Figure 8A). The presence of an additional band that was ~6 kDa smaller than the filaggrin trimer was also suggested. Therefore, in *B6Hai-1^{-/-High}* mice, profilaggrin processing was enhanced, whereas the generation of filaggrin monomer was severely impaired. We also performed primary culture of keratinocytes from newborn *B6Hai-1^{-/-High}* mice. In the isolated keratinocytes, Hai-1/Spint1 mRNA was undetectable with RT-PCR analysis (data not shown). As a control, keratinocytes from newborn *C57BL/6 Hai-1^{+/+}* mice were also isolated. Interestingly, enhanced processing and generation of abnormally processed filaggrin fragments were also observed in the extracts from detached cells in culture-conditioned medium of Hai-1/Spint1-deficient keratinocytes (Figure 8B). Casein zymography of the conditioned media revealed that increased activities of GM6001-resistant proteinase(s) in the conditioned media of Hai-1/Spint1-deficient keratinocytes (Figure 8C). These proteinase activities were phenylmethyl sulfonyl fluoride sensitive indicating that most of these caseinolytic bands represent serine proteinase activities (data not shown).

We then examined the processing of prostatic zymogen, which is mediated by matriptase,¹⁷ in skin tissues.

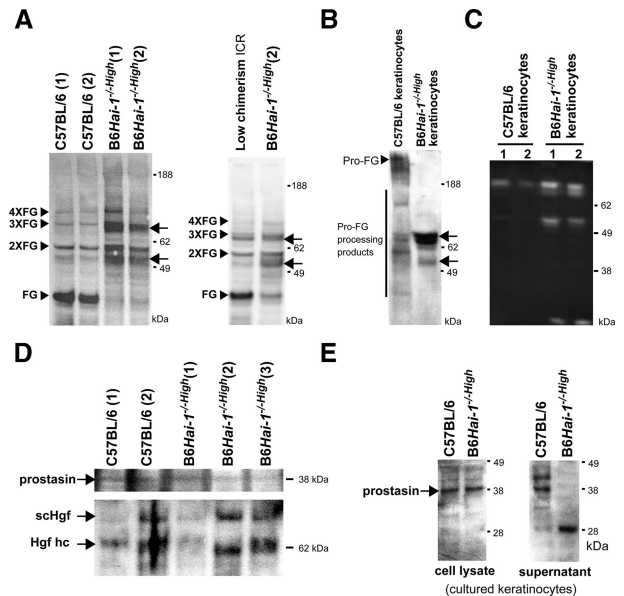


Figure 8. Altered filaggrin processing in keratinocytes of *B6Hai-1^{-/-High}* mice. **A:** Immunoblot analysis for profilaggrin processing in the skin. **Arrowheads** indicate the positions of filaggrin monomer (FG), dimer (2XFG), trimer (3XFG), and tetramer (4XFG). In the skin of *B6Hai-1^{-/-High}* mice, generation of filaggrin monomer was impaired, and abnormally processed filaggrin fragments (**arrows**) were detected. **B:** Immunoblot analysis for filaggrin of cultured keratinocytes. Cells were washed with serum-free, culture-conditioned medium and the detached cells and cellular debris were harvested, extracted with SDS sample buffer, and applied. The abnormally processed filaggrin fragments (**arrows**) were also observed in *B6Hai-1^{-/-High}* keratinocytes. **C:** Casein zymography of concentrated (20-fold) serum-free, culture-conditioned media of keratinocytes of similar cellular density in the presence of metalloprotease inhibitor GM6001. Enhanced caseinolytic activities of 70 to 90 kDa and 50 to 55 kDa were observed in *B6Hai-1^{-/-High}* keratinocytes. **D:** Immunoblot analysis of prostatic and Hgf in the skin tissue. Apparent alteration of prostatic processing was not observed in *B6Hai-1^{-/-High}* mice. Processing of inactive single-chain form of Hgf (scHgf) to active two-chain form was not apparently altered. Hgf hc, heavy chain of active two-chain Hgf. **E:** Immunoblot analysis of prostatic in whole cell extracts (lysate) and concentrated (20-fold) serum-free conditioned medium (supernatant) of cultured keratinocytes. In the conditioned medium, a 28-kDa fragment of prostatic was observed in Hai-1/Spint1-deficient keratinocytes.

As shown in Figure 8D, we could not detect apparent alteration of the prostatic processing in *B6Hai-1^{-/-High}* mouse skin *in vivo*. In cultured keratinocytes, the processing pattern of cellular prostatic did not apparently differ either. However, in the culture supernatant of Hai-1/Spint1-deficient keratinocytes, an abnormally processed 28-kDa band that was reactive to anti-prostatic monoclonal antibody was detected (Figure 8E). This 28-kDa band was not detectable in the whole skin extracts possibly because of low abundance of the protein. We also examined the processing of Hgf in the skin tissues, which might be mediated by serum Hgfa and/or cellular matriptase, both of which are sensitive to Hai-1/Spint1. The pattern of Hgf processing was not apparently altered in Hai-1/Spint1-deficient skin (Figure 8D).

Enhanced Phosphorylation of Akt in *Hai-1/Spint1*-Deficient Keratinocytes

A recent study revealed that transgenic overexpression of matriptase in keratinocytes results in the activation of Akt and skin carcinogenesis in a Hai-1/Spint1 inhibitable

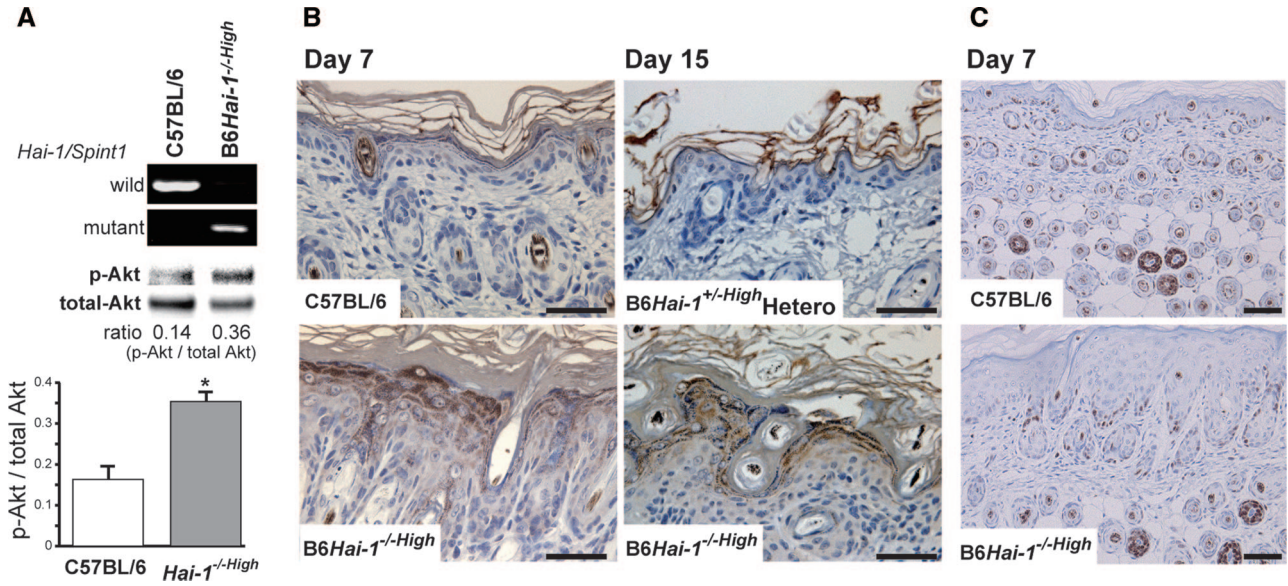


Figure 9. Enhanced phosphorylation of Akt in *Hai-1/Spint1*-deficient keratinocytes. **A:** Immunoblot analyses for phosphorylated Akt (p-Akt) of cultured keratinocytes. The same blot was reprobed with antibody against total Akt. The band intensity was measured and the ratio of p-Akt to the corresponding total Akt was calculated. The bar graph indicates means \pm SD of p-Akt/total Akt ratio ($n = 4$). $*P < 0.05$, Mann-Whitney U -test. The results of PCR genotyping of the keratinocytes are also shown. **B:** Immunohistochemistry for p-Akt. Enhanced immunoreactivity of p-Akt was observed in *Hai-1/Spint1*-deficient epidermal keratinocytes. **C:** Ki-67 immunoreactivity of the epidermis and hair follicles. Scale bars = 100 μ m.

manner.²⁰ Therefore, we examined the alteration of Akt phosphorylation in *Hai-1/Spint1*-deleted keratinocytes. The culture morphology was not altered significantly in B6*Hai-1*^{-/-High} keratinocytes except for showing a little more flattened shape compared with control keratinocytes (data not shown). Growth rate at the log phase was not altered either. On the other hand, immunoblot analysis of the cellular extracts revealed enhanced phosphorylation of Akt in cultured B6*Hai-1*^{-/-High} keratinocytes when compared with those from wild-type mice (Figure 9A). Enhanced Akt phosphorylation was also confirmed in the *in vivo* epidermis. Immunohistochemically, keratinocytes of B6*Hai-1*^{-/-High} mice showed significantly enhanced immunoreactivity of phospho-Akt relative to those of wild-type C57BL/6 and B6*Hai-1*^{+/-High} heterozygous mice (Figure 9B). However, follicular epithelial cells showed only mildly enhanced phospho-Akt immunoreactivity (data not shown). In contrast, the Ki-67 labeling index of keratinocytes was not altered by deletion of *Hai-1/Spint1* (Figure 9C).

Discussion

Targeted disruption of specific genes is a powerful tool for assessing gene function, and generation of knockout mice has been widely used as a conventional approach. However, the interpretation can be confounded by death of the mutant during development. Chimera analysis can offer a complementary approach to the assessment of phenotype.³¹ In this study, by using mouse embryo chimeras, we showed critical roles of *Hai-1/Spint1* in regulating keratinization of the epidermis and in normal development of hair and whiskers in mice. The results also confirmed our previous assumption that embryonic lethality of *Hai-1/Spint1* knockout mice was caused by im-

paired formation of the placental labyrinthine layer, not by abnormal embryo development.¹⁰

Regarding the placental defect in *Hai-1/Spint1*^{-/-} mice, recent reports have shown that interaction between *Hai-1/Spint1* and matriptase is critical, and the impaired development of the placental labyrinth in *Hai-1/Spint1*^{-/-} mice may be caused by an abnormal basement membrane possibly attributable to excess matriptase activity in trophoblasts.^{24,25} Prostatin, which is another target of *Hai-1/Spint1*¹³ and is activated by matriptase,¹⁷ may also be involved in this placental phenotype.²⁵ These observations in placenta morphogenesis indicate that interactions between *Hai-1/Spint1* and its cognate proteinases could have a critical role in the regulation of tissue development and homeostasis. Our present study has suggested that this is also the case in skin. In this study, we have shown that *Hai-1/Spint1* is strongly expressed in hair cortex and cuticle cells, and the defect of *Hai-1/Spint1* resulted in hair shaft abnormalities with impaired formation of regular layered cuticle structure. In the epidermis, *Hai-1/Spint1* was expressed in the upper spinous and granular layers, and the defect of *Hai-1/Spint1* resulted in hyperkeratinization, acanthosis, and reduced barrier function. These *Hai-1/Spint1*-positive keratinocytes are mostly nonproliferative cells and the expression pattern indicates that this inhibitor may be co-localized with matriptase in the hair follicle and with both matriptase and prostatin in the epidermis.^{28,29} Therefore, together with the observation that *matriptase/St14* knockout mice showed severe skin abnormalities such as abnormal barrier function and impaired hair follicle development,¹⁸ it is possible to speculate that there may be a critical interaction between *Hai-1/Spint1* and matriptase in the regulation of normal skin and hair development. However, the precise molecular mechanism underlying

the observed cuticle abnormality in *Hai-1/Spint1*-deleted hair and whisker remains to be determined and little is known regarding the role of matriptase in cuticle development. The critical interaction between Hai-1/Spint1 and matriptase has also been confirmed recently in zebrafish epidermis.³² The deletion of *Hai-1/Spint1* in zebrafish resulted in disrupted epidermal integrity, susceptibility to apoptosis in keratinocytes, and inflammation.^{32,33} Importantly, the epidermal phenotype of *Hai-1/Spint1*-deleted zebrafish was rescued by knockdown of matriptase.³²

The significant hyperkeratinization of the epidermis observed in *B6Hai-1^{-/-High}* mice is reminiscent of ichthyosis. Interestingly, a point mutation in *matriptase/ST14* causes autosomal recessive ichthyosis with hypotrichosis (ARIH).³⁴ In ARIH patients, the epidermis is thick and scaly, and hair shafts are irregular, flaky, and undulating.³⁴ Unlike common ichthyosis such as ichthyosis vulgaris, keratohyaline granules display normal features in ARIH.³⁴ These findings are quite similar to those observed in *B6Hai-1^{-/-High}* mice in this study. However, ARIH is caused by reduced activity of matriptase and can be phenocopied by matriptase hypomorphic mice.³⁵ Indeed, deletion of *matriptase/St14* in the skin results in the absence of filaggrin monomer,³⁰ and this defect of filaggrin maturation is mediated by impaired activation of prostaticin, a membrane-bound, Hai-1/Spint1-sensitive serine proteinase that is activated by matriptase.^{13,17,35} In this study, immunoblot analysis for filaggrin revealed abnormal processing of filaggrin in *B6Hai-1^{-/-High}* skin, showing impaired generation of filaggrin monomer with accumulation of filaggrin dimer and abnormally processed product that is 6 kDa smaller than the dimer. Surprisingly, this processing abnormality shows striking similarity to that observed in the *prostaticin/Prss8*-deleted skin.¹⁹ Therefore, despite the presumed overactivities of matriptase and prostaticin in the absence of Hai-1/Spint1, deletion of *Hai-1/Spint1* in the skin shows a similar phenotype to those observed in abnormally reduced matriptase or prostaticin activity, as if too much is as detrimental as too little. One possible explanation may be an existence of a Hai-1/Spint1-sensitive proteinase in keratinocytes, which may further degrade functional prostaticin protein. This hypothesis may be supported by the existence of abnormally processed lower-molecular weight prostaticin band in the culture supernatant of *Hai-1/Spint1*-deleted keratinocytes. Alternatively, as indicated in previous *in vitro* studies, Hai-1/Spint1 may be required in the physiological activation of promatriptase *in vivo*, and the formation of Hai-1/Spint1-matriptase complex might be critical for the translocation of matriptase to its proper destination on the cell surface where prostaticin zymogen is subsequently activated by matriptase.^{8,36} Whatever the mechanism may be, these findings suggest that tight regulation for optimal proteinase activity is critically required in maintaining regulated epidermal keratinization. On the other hand, although both matriptase- and prostaticin-deficient mice died from dehydration in early neonatal stages (within 60 hours) because of impaired epidermal barrier function, *B6Hai-1^{-/-High}* did not show fatal dehydration. The rate of fluid loss of *Hai-1/Spint1*-deleted skin was markedly lower than the

matriptase- or *prostaticin*-deleted mice, but was similar to that of matriptase hypomorphic mice.^{18,19,35}

The important role of proteinase-proteinase inhibitor balance in epidermal keratinization has also been shown in other proteinase/inhibitor systems.³⁷ A well known example is the *Spink5* knockout mouse, an animal model of Netherton syndrome characterized by ichthyosiform erythroderma, hair shaft abnormality, and severe atopic manifestation.^{38,39} SPINK5 is also a serine proteinase inhibitor and regulates the activities of stratum corneum tryptic enzyme and stratum corneum chymotryptic enzyme in the keratinocytes.^{38,39} However, in contrast to *Hai-1/Spint1* deletion, *Spink5* deletion showed enhanced generation of filaggrin monomer.³⁹ Therefore proteinase cascade regulated by Hai-1/Spint1 and *Spink5* might be distinct from each other in keratinocytes.

Of interest was the observation that *Hai-1/Spint1*-deleted keratinocytes showed enhanced phosphorylation of Akt, and the epidermis in *B6Hai-1^{-/-High}* showed an apparently thickened cell layer. The phosphatidylinositol 3-kinase (PI3K)-Akt pathway is dysregulated in a wide spectrum of human cancers.⁴⁰ In accordance with our findings, transgenic matriptase expression under keratin 5 promoter causes activation of the tumor-promoting PI3K-Akt in keratinocytes eventually resulting in squamous cell carcinoma in a Hai-1/Spint1-inhibitable manner.²⁰ Although the specific molecular events that underlie matriptase-induced activation of PI3K-Akt signaling axis remain unknown, these lines of evidence suggest uncontrolled excess matriptase activity in *Hai-1/Spint1*-deleted skin. Skin-specific conditional *Pten* knockout also resulted in phenotypes similar to our *B6Hai-1^{-/-High}* mice, showing up-regulation of Akt phosphorylation followed by epidermal hyperplasia with hyperkeratosis and ruffled, shaggy, and curly hair.⁴¹ In *Hai-1/Spint1*-deleted zebrafish, epidermal hyperproliferation occurs in later periods.^{32,33} Taken altogether, disturbance of the balance of Hai-1/Spint1 and its cognate proteinase, such as matriptase, leads to deranged intracellular signaling and a proliferative skin disease. In this regard, Hai-1/Spint1 may be a tumor suppressor. On the other hand, despite apparent acanthosis of the epidermis in Hai-1/Spint1-deficient mice, Ki-67 labeling index of keratinocytes was not increased significantly, and mechanism underlying the thickened epidermal layer remains to be clarified.

An important question unanswered in this study is the cause of lethality of *B6Hai-1^{-/-High}* pups. Several days after birth, growth retardation became apparent and *B6Hai-1^{-/-High}* mice died by 16 days after birth. One possible explanation for this growth retardation may be considerable hyperkeratinization of the forestomach stratified squamous epithelium in *B6Hai-1^{-/-High}* mice, which would disturb milk intake. Similar to our observation, the *k5Ptenflox/flox* mice also die of malnutrition caused by hyperkeratosis of the esophagus within 3 weeks of birth.⁴¹ *Keap-1* knockout mice also show ichthyosis-like scaling skin and die from malnutrition caused by hyperkeratinization of esophagus and forestomach mucosae.⁴² Alternatively, because Hai-1/Spint1 is also strongly expressed in most columnar epithelial cells covering the mucosal surface of the gastrointestinal tract,

deletion of Hai-1/Spint1 might somehow cause disastrous effects on the absorption function of the epithelium. The chimera strategy used in this study is technically tedious and has striking limitations to prepare many pups of similar condition. Clearly, for better understanding of the lethality observed in this study and to investigate the roles of Hai-1/Spint1 in various organs such as gastrointestinal tracts, a conditional gene targeting strategy would be required.

In summary, Hai-1/Spint1 has important roles in epidermal keratinization and hair development. These functions of Hai-1/Spint1 in the skin may be related to the interaction with its target proteinases, matriptase and prostasin. However, this study also indicates the complexity of proteinase/inhibitor interactions involved in regulating epidermal keratinization, and suggests that tight regulation for the optimal proteinase activity by its cognate inhibitor is critical. Finally, although Hai-1/Spint1 function appears to be redundant with other inhibitors during development of the embryo body, Hai-1/Spint1 may have essential roles in the maintenance of physiological homeostasis, which is required in the growth and survival of newborn mice, because *B6Hai-1^{-/-}High* pups died within 16 days of birth.

Acknowledgments

We thank Dr. Gen Yamada (Center for Animal Resources and Development, Graduate School of Molecular and Genomic Pharmacy, Kumamoto University, Kumamoto, Japan) for helpful suggestions and Ms. Yasuko Tobayashi and Yukari Kawagoe for their excellent technical assistance.

References

1. Shimomura T, Denda K, Kitamura A, Kawaguchi T, Kito M, Kondo J, Kagaya S, Qin L, Takata H, Miyazawa K, Kitamura K: Hepatocyte growth factor activator inhibitor, a novel Kunitz-type serine protease inhibitor. *J Biol Chem* 1997, 272:6370–6376
2. Kataoka H, Miyata S, Uchinokura S, Itoh H: Roles of hepatocyte growth factor (HGF) activator and HGF activator inhibitor in the pericellular activation of HGF/scatter factor. *Cancer Metastasis Rev* 2003, 22:223–236
3. Kataoka H, Suganuma T, Shimomura T, Itoh H, Kitamura N, Nabeshima K, Koono M: Distribution of hepatocyte growth factor activator inhibitor type 1 (HAI-1) in human tissues: cellular surface localization of HAI-1 in simple columnar epithelium and its modulated expression in injured and regenerative tissues. *J Histochem Cytochem* 1999, 47:673–682
4. Oberst M, Anders J, Xie B, Singh B, Ossandon M, Johnson M, Dickson RB, Lin CY: Matriptase and HAI-1 are expressed by normal and malignant epithelial cells in vitro and in vivo. *Am J Pathol* 2001, 158:1301–1311
5. Kataoka H, Meng JY, Itoh H, Hamasuna R, Shimomura T, Suganuma T, Koono M: Localization of hepatocyte growth factor activator inhibitor type 1 in Langhans' cells of human placenta. *Histochem Cell Biol* 2000, 114:469–475
6. Akiyama Y, Nagai M, Komaki W, Marutsuka K, Asada Y, Kataoka H: Expression of hepatocyte growth factor activator inhibitor type 1 in endothelial cells. *Human Cell* 2006, 19:91–97
7. Kataoka H, Shimomura T, Kawaguchi T, Hamasuna R, Itoh H, Kitamura N, Miyazawa K, Koono M: Hepatocyte growth factor activator inhibitor type 1 is a specific cell surface binding protein of hepatocyte growth factor activator (HGFA) and regulates HGFA activity in the pericellular microenvironment. *J Biol Chem* 2000, 275:40453–40462
8. Oberst MD, Chen LY, Kiyomiya KI, Williams CA, Lee MS, Johnson MD, Dickson RB, Lin CY: Hepatocyte growth factor activator inhibitor 1 (HAI-1) regulates activation and expression of matriptase, a membrane-bound serine protease. *Am J Physiol* 2005, 289:C462–C470
9. List K, Bugge TH, Szabo R: Matriptase: potent proteolysis on the cell surface. *Mol Med* 2006, 12:1–7
10. Tanaka H, Nagaike K, Takeda N, Itoh H, Kohama K, Fukushima T, Miyata S, Uchiyama S, Uchinokura S, Shimomura T, Miyazawa K, Kitamura N, Yamada G, Kataoka H: Hepatocyte growth factor activator inhibitor type 1 (HAI-1) is required for branching morphogenesis in the chorioallantoic placenta. *Mol Cell Biol* 2005, 25:5687–5698
11. Denda K, Shimomura T, Kawaguchi T, Miyazawa K, Kitamura N: Functional characterization of Kunitz domains in hepatocyte growth factor activator inhibitor type 1. *J Biol Chem* 2002, 277:14053–14059
12. Lin CY, Anders J, Johnson M, Dickson RB: Purification and characterization of a complex containing matriptase and a Kunitz-type serine protease inhibitor from human milk. *J Biol Chem* 1999, 274:18237–18242
13. Fan B, Wu TD, Li W, Kirchhofer D: Identification of hepatocyte growth factor activator inhibitor-1B as a potential physiological inhibitor of prostasin. *J Biol Chem* 2005, 280:34513–34520
14. Kirchhofer D, Peek M, Lipari MT, Billeci K, Fan B, Moran P: Hepsin activates pro-hepatocyte growth factor and is inhibited by hepatocyte growth factor activator inhibitor-1B (HAI-1B) and HAI-2. *FEBS Lett* 2005, 579:1945–1950
15. Miyazawa K, Shimomura T, Kitamura A, Kondo J, Morimoto Y, Kitamura N: Molecular cloning and sequence analysis of the cDNA for a human serine protease responsible for activation of hepatocyte growth factor. Structural similarity of the protease precursor to blood coagulation factor XII. *J Biol Chem* 1993, 268:10024–10028
16. Netzel-Arnett S, Hooper JD, Szabo R, Madison EL, Quigley JP, Bugge TH, Antalis TM: Membrane anchored serine proteases: a rapidly expanding group of cell surface proteolytic enzymes with potential roles in cancer. *Cancer Metastasis Rev* 2003, 22:237–258
17. Netzel-Arnett S, Currie BM, Szabo R, Lin CY, Chen LM, Chai KX, Antalis TM, Bugge TH, List K: Evidence for a matriptase-prostasin proteolytic cascade regulating terminal epidermal differentiation. *J Biol Chem* 2006, 281:32941–32945
18. List K, Haudenschild CC, Szabo R, Chen W, Wahl SM, Swaim W, Engelholm LH, Behrendt N, Bugge TH: Matriptase/MT-SP1 is required for postnatal survival, epidermal barrier function, hair follicle development, and thymic homeostasis. *Oncogene* 2002, 21:3765–3779
19. Leyvraz C, Charles RP, Rubera I, Guitard M, Rotman S, Breiden B, Sandhoff K, Hummler E: The epidermal barrier function is dependent on the serine protease CAP1/Prss8. *J Cell Biol* 2005, 170:487–496
20. List K, Szabo R, Molinolo A, Sriuranpong V, Redeye V, Murdock T, Burke B, Nielsen BS, Gutkind JS, Bugge TH: Deregulated matriptase causes ras-independent multistage carcinogenesis and promotes ras-mediated malignant transformation. *Genes Dev* 2005, 19:1934–1950
21. Oberst MD, Johnson MD, Dickson RB, Lin CY, Singh B, Stewart M, Williams A, al-Nafussi A, Smyth JF, Gabra H, Sellar GC: Expression of the serine protease matriptase and its inhibitor HAI-1 in epithelial ovarian cancer: correlation with clinical outcome and tumor clinicopathological parameters. *Clin Cancer Res* 2002, 8:1101–1107
22. Klezovitch O, Chevillet J, Mirosevich J, Roberts RL, Matusik RJ, Vasioukhin V: Hepsin promotes prostate cancer progression and metastasis. *Cancer Cell* 2004, 6:185–195
23. Betsunoh H, Mukai S, Akiyama Y, Fukushima T, Minamiguchi N, Hasui Y, Osada Y, Kataoka H: Clinical relevance of hepsin and hepatocyte growth factor activator inhibitor type 2 expression in renal cell carcinoma. *Cancer Sci* 2007, 98:491–498
24. Szabo R, Molinolo A, List K, Bugge TH: Matriptase inhibition by hepatocyte growth factor activator inhibitor-1 is essential for placental development. *Oncogene* 2007, 26:1546–1556
25. Fan B, Brennan J, Grant D, Peale F, Rangell L, Kirchhofer D: Hepatocyte growth factor activator inhibitor-1 (HAI-1) is essential for the integrity of basement membranes in the developing placental labyrinth. *Dev Biol* 2007, 303:222–230
26. Nagaike K, Kohama K, Uchiyama S, Tanaka H, Chijiwa K, Itoh H, Kataoka H: Paradoxically enhanced immunoreactivity of hepatocyte growth factor activator inhibitor type 1 (HAI-1) in cancer cells at the invasion front. *Cancer Sci* 2004, 95:728–735

27. Hager B, Bickenbach JR, Fleckman P: Long-term culture of murine epidermal keratinocytes. *J Invest Dermatol* 1999, 112:971–976
28. List K, Szabo R, Molinolo A, Nielsen BS, Bugge TH: Delineation of matriptase protein expression by enzymatic gene trapping suggests diverging roles in barrier function, hair formation, and squamous cell carcinogenesis. *Am J Pathol* 2006, 168:1513–1525
29. List K, Hobson JP, Molinolo A, Bugge TH: Co-localization of the channel activating protease prostatic/CAP1/PRSS8 with its candidate activator, matriptase. *J Cell Physiol* 2007, 213:237–245
30. List K, Szabo R, Wertz PW, Segre J, Haudenschild CC, Kim SY, Bugge TH: Loss of proteolytically processed filaggrin caused by epidermal deletion of matriptase/MT-SP1. *J Cell Biol* 2003, 163:901–910
31. Tam PPL, Rossant J: Mouse embryonic chimeras: tools for studying mammalian development. *Development* 2003, 130:6155–6163
32. Carney TJ, von der Hardt S, Sonntag C, Amsterdam A, Topczewski J, Hopkins N, Hammerschmidt M: Inactivation of serine protease matriptase 1a by its inhibitor Hai1 is required for epithelial integrity of the zebrafish epidermis. *Development* 2007, 134:3461–3471
33. Mathias JR, Dodd ME, Walters KB, Rhodes J, Kanki JP, Look AT, Huttenlocher A: Live imaging of chronic inflammation caused by mutation of zebrafish Hai1. *J Cell Sci* 2007, 120:3372–3383
34. Basel-Vanagaite L, Attia R, Ishida-Yamamoto A, Rainshtein L, Ben Amitai D, Lurie R, Pasmanik-Chor M, Indelman M, Zvulunov A, Saban S, Magal N, Sprecher E, Shohat M: Autosomal recessive ichthyosis with hypotrichosis caused by a mutation in ST14, encoding type II transmembrane serine protease matriptase. *Am J Hum Genet* 2007, 80:467–477
35. List K, Currie B, Scharschmidt TC, Szabo R, Shireman J, Molinolo A, Cravatt BF, Segre J, Bugge TH: Autosomal ichthyosis with hypotrichosis syndrome displays low matriptase proteolytic activity and is phenocopied in ST14 hypomorphic mice. *J Biol Chem* 2007, 282:36714–36723
36. Lee MS, Tseng IC, Wang Y, Kiyomiya KI, Johnson MD, Dickson RB, Lin CY: Autoactivation of matriptase in vitro: requirement for biomembrane and LDL receptor domain. *Am J Physiol* 2007, 293:C95–C105
37. Zeeuwen PLJM: Epidermal differentiation: the role of proteases and their inhibitors. *Eur J Cell Biol* 2004, 83:761–773
38. Yang T, Liang D, Koch PJ, Hohl D, Kheradmand F, Overbeek PA: Epidermal detachment, desmosomal dissociation, and destabilization of corneodesmosin in Spink5^{-/-} mice. *Genes Dev* 2004, 18:2354–2358
39. Descargues P, Deraison C, Bonnart C, Kreft M, Kishibe M, Ishida-Yamamoto A, Elias P, Barrandon Y, Zambruno G, Sonnenberg A, Hovnanian A: Spink5-deficient mice mimic Netherton syndrome through degradation of desmoglein 1 by epidermal protease hyperactivity. *Nat Genet* 2005, 37:56–65
40. Fresno Vara JA, Casado E, de Castro J, Cejas P, Belda-Iniesta C, González-Barón M: PI3K/Akt signalling pathway and cancer. *Cancer Treat Rev* 2004, 30:193–204
41. Suzuki A, Itami S, Ohishi M, Hamada K, Inoue T, Komazawa N, Senoo H, Sasaki T, Takeda J, Manabe M, Mak TW, Nakano T: Keratinocyte-specific Pten deficiency results in epidermal hyperplasia, accelerated hair follicle morphogenesis and tumor formation. *Cancer Res* 2003, 63:674–681
42. Wakabayashi N, Itoh K, Wakabayashi J, Motohashi H, Noda S, Takahashi S, Imakado S, Kotsuji T, Otsuka F, Roop DR, Harada T, Engel JD, Yamamoto M: Keap1-null mutation leads to postnatal lethality due to constitutive Nrf2 activation. *Nat Genet* 2003, 35:238–245